A comparison of scale-dependent Joule heating rate estimates from two sets of sounding rocket measurements in disturbed auroral conditions

L. D. Hurd[1], M. F. Larsen[1], R. F. Pfaff[2]

Introduction

- The contribution of electric field variability to high-latitude Joule heating estimates has been studied in some detail using ground-based radar and various modeling schemes [see, e.g., *Codrescu et al.* (2000), *Cosgrove et al.* (2009), *Cousins and Shepherd* (2012)], but at what scale the variability becomes important is still an outstanding question.
- Experimental studies of the neutral wind effects on the *E* region Joule heating are limited.
- The JOULE-1 and JOULE-2 rocket campaigns were carried out to assess the importance of small-scale electrodynamic structure on the Joule heating rate in the high-latitude *E* region during a substorm.
- The rockets provided *in-situ* measurements of the electric field using electric field double probes, the electron density using Langmuir probes, and the neutral wind by tracking trimethyl aluminum (TMA) releases, with spatial resolutions better than 1 km for all observations.

Method

Following a similar approach as *Cosgrove et al.* (2009), start with the field-line integrated Joule heating rate, *J*, including the neutral wind,

$$J = \Sigma_P \left(\left|\vec{E}\right|^2 + \left|\vec{U}\times\vec{B}\right|^2 + 2\vec{E}\cdot\left(\vec{U}\times\vec{B}\right) \right) \quad (1)$$

making the usual assumptions that the field-aligned current and the neutral vertical velocity are small, so that we only consider the perpendicular electric field and horizontal neutral wind. Σ_P is the Pedersen conductance. The electric field can be written as the sum of its mean and fluctuating components,

$$\vec{E} = \langle\vec{E}\rangle + \vec{E}'. \quad (2)$$

We will only consider spatial fluctuations here, so that the mean of the fluctuating component is zero over the spatial domain of the measurements. To make comparisons between data sets with varying resolutions, substitute (2) into (1) and take the mean over the full expression:

$$\langle J\rangle = \underbrace{\langle\Sigma_P\rangle\left|\langle\vec{E}\rangle\right|^2}_{\textbf{Term 1}} + \underbrace{\langle\Sigma_P\rangle\langle\left|\vec{E}'\right|^2\rangle}_{\textbf{Term 2}} + \underbrace{\langle\Sigma_P\rangle\langle\left|\vec{U}\times\vec{B}\right|^2\rangle}_{\textbf{Term 3A}} + \underbrace{2\langle\Sigma_P\rangle\langle\vec{E}\rangle\cdot\langle\vec{U}\times\vec{B}\rangle}_{\textbf{Term 3B}}. \quad (3)$$

Term 1 is the contribution to the Joule heating due to the squared mean electric field. Term 2 is the contribution from the small-scale variability in the electric field. The sum of Terms 3A and 3B is the contribution from neutral wind effects. The spatial range over which we resolve the mean values is variable up to the instantaneous resolution of the rocket measurements.

JOULE-1

- Two pairs of sounding rockets were launched 6 min apart along two different trajectories on 27 March 2003 at 1209 UT (0309 LT) from the Poker Flat Research Range in Alaska.
- Each pair included an instrumented rocket to measure the electrodynamic parameters and a chemical tracer rocket launched along a similar trajectory to measure the neutral winds.
- The rocket pairs were launched nearly simultaneously along different trajectories to observe the spatial variations in the electric field.
- The Kp index reached 5- on the day of the experiment and data from the Alaskan magnetometer chain showed negative deflections in the *H* component of 400 nT above Poker Flat.

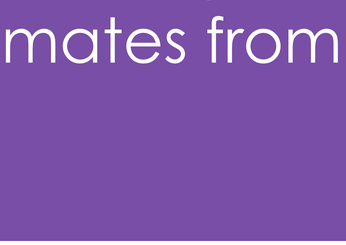

Figure 1 (above): RGB keogram from the Poker Flat meridian scanning photometer for the evening of the JOULE-1 experiment.

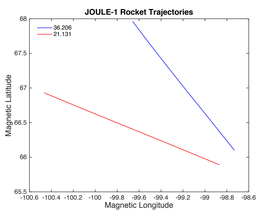

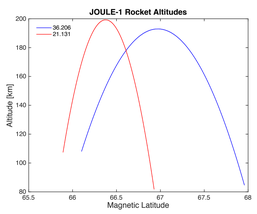

Figure 2 (left): Trajectories and altitudes of the data coverage for the two JOULE-1 instrumentation rockets.

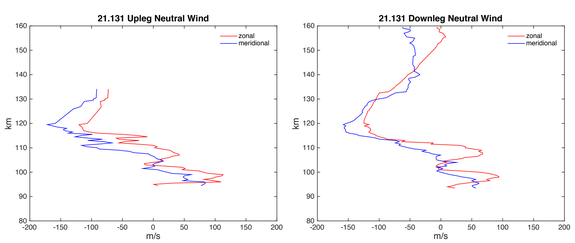

Figure 3 (right): Neutral wind components derived from TMA releases for one of the JOULE-1 chemical tracer rockets.

[1] Department of Physics and Astronomy, Clemson University, Clemson, SC, USA (lhurd@clemson.edu)
[2] NASA Goddard Space Flight Center, Greenbelt, MD, USA

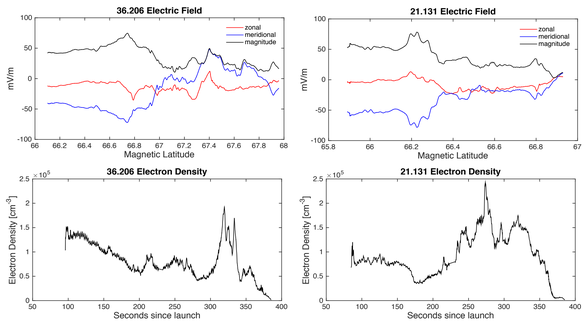

Figure 4 (right): Electric fields and electron densities observed by the JOULE-1 flights.

- The neutral wind and electron density profiles are treated as two point measurements horizontally separated, and we assume that variations between the profiles at the same altitudes are linear.
- For JOULE-1, the second-stage ignition failed on the first chemical tracer rocket, so the complete horizontal gradients in the neutral wind field were not observed.
- The interpolated electron density observations are used to estimate the Pedersen conductivity using NRLMSISE-00 and IRI-2012 to obtain the constituent number densities required for the calculations.
- The magnetic field values for all of the calculations are taken from IGRF.
- We assume that the electric field maps along the magnetic field lines and carry out the integrated Joule heating estimates for 95 to 135 km in altitude.

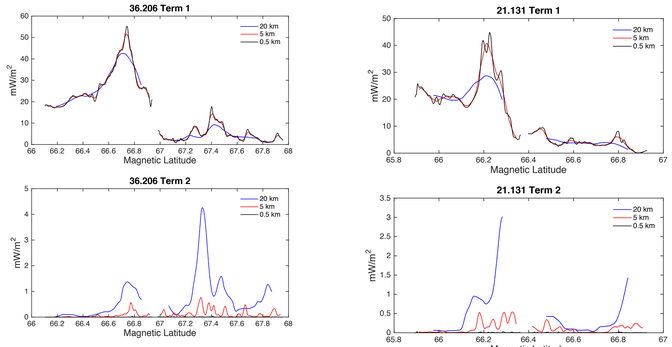

Figure 5: (above) Heating contributions from the terms in equation (3) for 36.206. The legend refers to the spatial resolution of the calculations. The neutral wind terms could not be calculated for this case. (right) Same as above, except for 21.131. The neutral wind terms are evaluated in this case – i.e., Term 3 is the sum of Terms 3A and 3B.

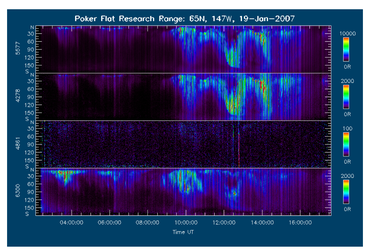

Figure 6 (above): RGB keogram from the Poker Flat meridian scanning photometer for the evening of the JOULE-2 experiment.

JOULE-2

- Two pairs of sounding rockets were launched 15 min apart along similar trajectories on 19 January 2007 at 1229 UT (0329 LT) from Poker Flat.
- As in JOULE-1, each pair included an instrumented and chemical tracer rocket.
- The rocket pairs were launched along similar trajectories in this case to observe the temporal evolution of the electric field.
- The Kp index reached 4 on the day of the experiment and the magnetometers showed negative deflections in the *H* component of over 400 nT above Poker Flat.

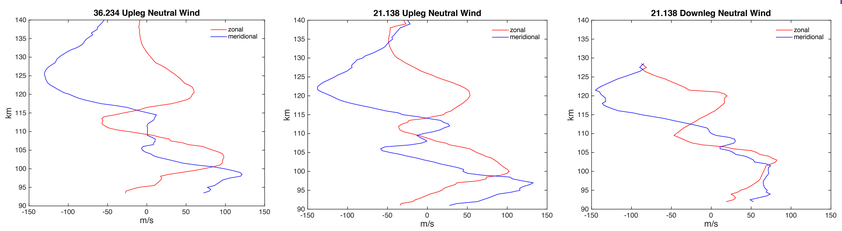

Figure 7 (above): Neutral wind components derived from TMA releases for JOULE-2. The downleg payload corresponding to 36.234 failed to deploy, so we assume that the wind field is constant for the upleg portion of that flight for the Joule heating estimates.

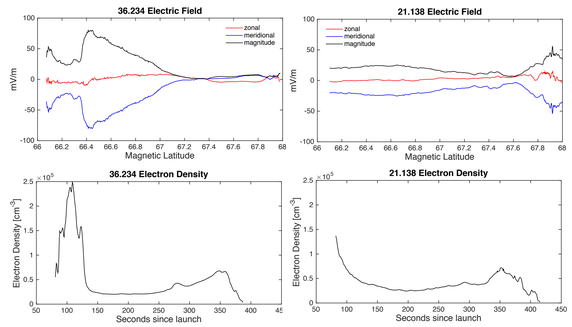

Figure 8 (left): Electric fields and electron densities observed by the JOULE-2 flights.

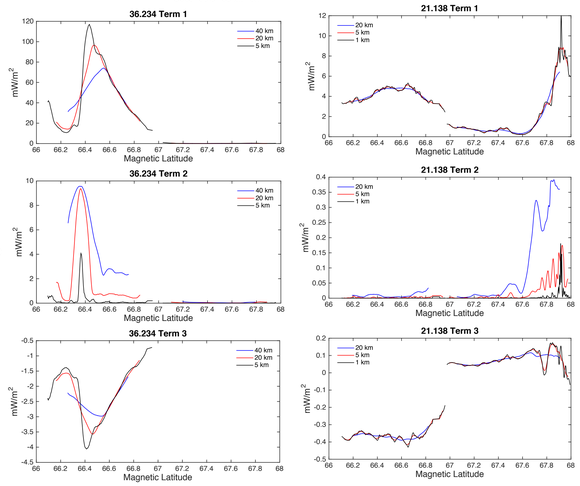

Figure 9 (right): Heating contributions from the terms in equation (3) for the JOULE-2 flights. The neutral wind terms could only be calculated for the upleg portion of 36.234.

Conclusions

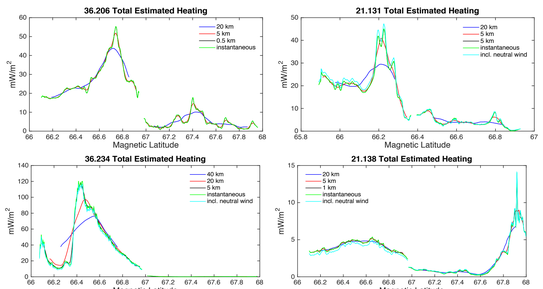

Figure 10 (left): Total estimated heating for various resolutions and the instantaneous heating, both excluding and including the neutral wind, calculated at each sampled point for all four rocket pairs considered here.

- The rocket measurements indicate that during moderately active conditions, the Joule heating rate is evolving rapidly in both space and time on scales of tens of km in only a few min.
- The small-scale variability is most important near auroral structures, and becomes increasingly important as the resolution of the heating calculations are degraded.
- Electric field structure on scales down to 5 km contributes significantly to the overall Joule heating.
- For 20 km resolution, the heating is consistently underestimated by up to 50% compared to the instantaneous heating.
- The neutral wind field was shown to be relatively constant throughout the observation regions, while the electrodynamic parameters vary significantly on the scales considered here.
- Including the neutral wind in the heating calculations serves to both increase and decrease the estimated integrated heating by up to 10% at times.
- *Cosgrove et al.* (2011) also showed that degrading the resolution of the measurements results in an overall underestimation of the heating, but the rocket data specifically show that to accurately estimate the Joule heating rate, measurements or models need to be able to resolve the electric field on scales down to 5 km, at least for these two cases.

Acknowledgements

L.D.H. gratefully acknowledges support by NASA Headquarters under the NASA Earth and Space Science Fellowship Program under grant NNX13AM28H.

References

Codrescu, M. V., T. J. Fuller-Rowell, J. C. Foster, J. M. Holt, and S. J. Cariglia (2000), Electric field variability associated with the Millstone Hill electric field model, *J. Geophys. Res.*, *105*(A3), 5265, doi: 10.1029/1999JA900463.
Cosgrove, R. B., G. Lu, H. Bahcivan, T. Matsuo, C. J. Heinselman, and M. A. McCready (2009), Comparison of AMIE-modeled and Sondrestrom-measured Joule heating: a study in model resolution and electric field-conductivity correlation, *J. Geophys. Res.*, *114*, A04316, doi: 10.1029/2008JA013508.
Cosgrove, R., M. McCready, R. Tsunoda, and A. Stromme (2011), The bias on the Joule heating estimate: small-scale variability versus resolved-scale model uncertainty and the correlation of electric field and conductance, *J. Geophys. Res.*, *116*, A09320, doi: 10.1029/2011JA016665.
Cousins, E. D. P. and S. G. Shepherd (2012), Statistical characteristics of small-scale spatial and temporal electric field variability in the high-latitude ionosphere, *J. Geophys. Res.*, *117*, A03317, doi: 10.1029/2011JA017383.